A rotational hardening model applicable to finite strain analysis based on multiplicative decomposition of plastic deformation gradient tensor

Keita Nakamura[1] and M. Kikumoto[2]

[1] Port and Airport Research Institute, Yokosuka, Japan.
[2] Department of Civil Engineering, Yokohama National University, Yokohama, Japan.

ABSTRACT

A rotational hardening model applicable to finite strain analysis based on the multiplicative decomposition of plastic deformation gradient tensor is presented, based on the framework proposed by Lion (2000). In the formulation, a new description of back stress is proposed to incorporate the Armstrong–Frederick kinematic hardening law into the rotational hardening law for soils. The validity of the proposed model is confirmed by stress-controlled cyclic simple shearing simulations.

Keywords: stress-induced anisotropy; Cam-clay; rotational hardening; Armstrong–Frederick kinematic hardening; finite strain analysis

1 INTRODUCTION

Soil behavior is strongly affected by induced anisotropy that evolves owing to past stress histories such as the cyclic loading or rotation of principal stress axes, and it needs to be properly described by a constitutive model for soils. In addition, the deformation and failure of soil such as those caused by an earthquake tend to be large, and it should be simulated based on a theory that incorporates geometric nonlinearity such as the finite strain theory. Hence, Lion (2000) developed a finite strain framework that incorporates stress-induced anisotropy by employing an additional multiplicative split of the plastic part of the deformation gradient into the elastic and inelastic parts based on the kinematic hardening law of Armstrong and Frederick (1966). This framework has several advantages over the existing "Chaboche-type" models requiring the derivation of an evolution equation for the back stress (see, e.g., Dettmer and Stefanie, 2004).

However, the existing studies (e.g., Chida et al., 2013) to verify whether this framework is applicable for modeling anisotropic behavior of soils are scarce. We thus derive an infinitesimal model (not finite strain model to avoid complexities in the formulation) that can easily be extended to the finite strain framework proposed by Lion (2000) as follows: (1) the plastic part of the infinitesimal strain is split additively into elastic and inelastic parts; (2) the free energy function is divided into the hyperelastic part and hardening part including isotropic and rotational hardening laws; (3) the hardening part is formulated based on the kinematic hardening law of Armstrong and Frederick (1966); (4) the flow rules are defined to satisfy the thermodynamics restrictions.

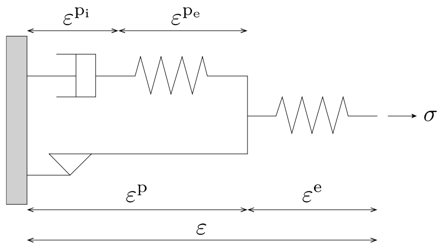

Fig. 1. Rheological model of Armstrong and Frederick (1966) kinematic hardening.

2 DESCRIPTION OF BACK STRESS

A new description of the back stress that can describe both the isotropic and rotational hardening laws is presented herein.

The finite strain framework for an anisotropic material (Lion, 2000) is based on the one-dimensional Armstrong–Frederick rheology model as shown in Fig. 1; it shows that the plastic part of the infinitesimal strain is further split additively into the elastic and inelastic parts:

$$\boldsymbol{\varepsilon} = \boldsymbol{\varepsilon}^{\mathrm{e}} + \boldsymbol{\varepsilon}^{\mathrm{p}} = \boldsymbol{\varepsilon}^{\mathrm{e}} + \boldsymbol{\varepsilon}^{\mathrm{p_e}} + \boldsymbol{\varepsilon}^{\mathrm{p_i}} \tag{1}$$

where $\boldsymbol{\varepsilon}^{\mathrm{p_e}}$ and $\boldsymbol{\varepsilon}^{\mathrm{p_i}}$ are the elastic and inelastic parts of the plastic strain $\boldsymbol{\varepsilon}^{\mathrm{p}}$, respectively.

In the Armstrong–Frederick kinematic hardening law, anisotropy is expressed by a back stress $\boldsymbol{\chi}$ that is a work-conjugate stress to the inelastic part of the plastic strain $\boldsymbol{\varepsilon}^{\mathrm{p_i}}$. However, this is inconsistent with the rotational hardening law as it applies a nondimensional rotation of axis of the yield surface as an internal variable. Meanwhile, in this study, we utilize the center of the yield surface as the back stress $\boldsymbol{\chi}$ and vary the back stress while maintaining the origin of the yield surface, as shown in Fig. 2. Here, the stress-like variable related with isotropic hardening (preconsolidation pressure p_c) and the variable related with rotational hardening (rotational axis $\overline{\boldsymbol{\eta}}$) are given as follows:

$$p_c = 2\bar{p} = 2\mathrm{tr}(\boldsymbol{\chi})/3, \qquad \overline{\boldsymbol{\eta}} = \mathrm{dev}(\boldsymbol{\chi})/\bar{p} \tag{2}$$

3 HYPERELASTO-PLASTIC CONSTITUTIVE MODEL

We formulate a hyperelasto-plastic model that satisfies the dissipation inequality.

3.1 Helmholtz free energy

The Helmholtz free energy function is defined as

$$\psi(\boldsymbol{\varepsilon}^{\mathrm{e}}, \boldsymbol{\varepsilon}^{\mathrm{p_e}}) \coloneqq W(\boldsymbol{\varepsilon}^{\mathrm{e}}) + \mathcal{H}(\boldsymbol{\varepsilon}^{\mathrm{p_e}}) \tag{3}$$

where W and $\mathcal{H}$ are the functions for the hyperelastic model and isotropic-rotational hardening law, respectively. From Eq. (3), the dissipation inequality is given as

$$\begin{aligned}\mathcal{D} &= \boldsymbol{\sigma}:\dot{\boldsymbol{\varepsilon}} - \dot{\psi} \\ &= \left(\boldsymbol{\sigma} - \frac{\partial W}{\partial \boldsymbol{\varepsilon}^{\mathrm{e}}}\right):\dot{\boldsymbol{\varepsilon}} + \left(\frac{\partial W}{\partial \boldsymbol{\varepsilon}^{\mathrm{e}}} - \frac{\partial \mathcal{H}}{\partial \boldsymbol{\varepsilon}^{\mathrm{p_e}}}\right):\dot{\boldsymbol{\varepsilon}}^{\mathrm{p}} + \frac{\partial \mathcal{H}}{\partial \boldsymbol{\varepsilon}^{\mathrm{p_e}}}:\dot{\boldsymbol{\varepsilon}}^{\mathrm{p_i}} \\ &= (\boldsymbol{\sigma} - \boldsymbol{\chi}):\dot{\boldsymbol{\varepsilon}}^{\mathrm{p}} + \boldsymbol{\chi}:\dot{\boldsymbol{\varepsilon}}^{\mathrm{p_i}} \geq 0\end{aligned} \tag{4}$$

where the hyperelastic constitutive model is given as

$$\boldsymbol{\sigma} = \frac{\partial W}{\partial \boldsymbol{\varepsilon}^{\mathrm{e}}} = \nabla W(\boldsymbol{\varepsilon}^{\mathrm{e}}) \tag{5}$$

and the back stress $\boldsymbol{\chi}$ for the isotropic-rotational hardening law is defined as

$$\boldsymbol{\chi} \coloneqq \frac{\partial \mathcal{H}}{\partial \boldsymbol{\varepsilon}^{\mathrm{p_e}}} = \nabla \mathcal{H}(\varepsilon^{\mathrm{p_e}}). \tag{6}$$

3.2 Yield function and flow rules

The flow rules for ε^{p} and $\varepsilon^{\mathrm{p_i}}$ are defined to satisfy $\mathcal{D} \geq 0$ as

$$\boldsymbol{\varepsilon}^{\mathrm{p}} = \dot{\gamma}\frac{\partial f}{\partial \boldsymbol{\sigma}} \Big/ \left\|\frac{\partial f}{\partial \boldsymbol{\sigma}}\right\|, \qquad \boldsymbol{\varepsilon}^{\mathrm{p_i}} = \dot{\gamma}\frac{\overline{\boldsymbol{\eta}}}{\overline{m}} = \dot{\gamma}\overline{\boldsymbol{N}} \tag{7}$$

where $\overline{m}$ is a positive material parameter. f is the yield function that can describe the isotropic and rotational hardening, as shown in Fig. 2. In this study, we employ a form proposed by Dafalias (1986):

$$f(\boldsymbol{\sigma}, \boldsymbol{\chi}) \coloneqq \frac{\|\boldsymbol{\eta} - \overline{\boldsymbol{\eta}}\|^2}{m^2 - \|\overline{\boldsymbol{\eta}}\|^2} + 1 - \frac{2\bar{p}}{p} \tag{8}$$

where $\boldsymbol{\eta} = \mathrm{dev}(\boldsymbol{\sigma})/p$ and m is the critical stress ratio.

3.3 Hyperelastic model

As a potential function, we propose the following equation:

$$W(\boldsymbol{\varepsilon}^{\mathrm{e}}) \coloneqq \tilde{\kappa} p_{\mathrm{ref}} \exp\Omega + \mu_{\mathrm{ref}}\boldsymbol{e}^{\mathrm{e}}:\boldsymbol{e}^{\mathrm{e}} \tag{9}$$

where

$$\Omega \coloneqq \frac{\varepsilon_{\mathrm{v}}^{\mathrm{e}}}{\tilde{\kappa}} + \frac{\alpha}{\tilde{\kappa}}\boldsymbol{e}^{\mathrm{e}}:\boldsymbol{e}^{\mathrm{e}} \tag{10}$$

$\tilde{\kappa}$ is the swelling index in the $\ln p$–$\ln v$ space (v, the specific volume; p, the mean stress), p_{ref} is the reference pressure at $\varepsilon_{\mathrm{v}}^{\mathrm{e}} = 0$, μ_{ref} is the shear modulus,

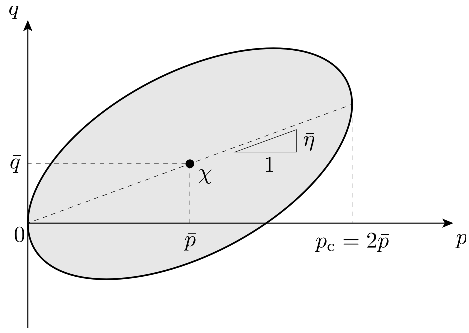

Fig. 2. Description of the isotropic and rotational hardening based on the back stress.

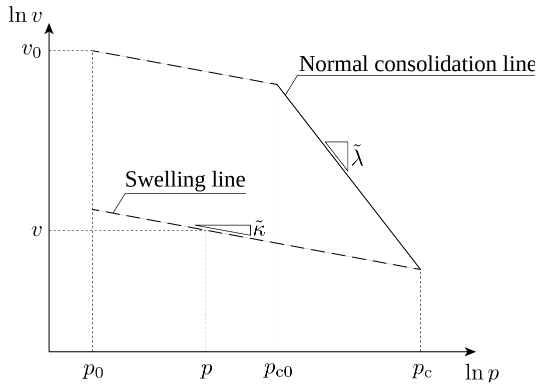

Fig. 3. Consolidation lines of the linear bi-logarithmic relation.

and α is a volumetric–deviatoric coupling parameter. If $\alpha > 0$ and $\mu_{\mathrm{ref}} = 0$, then the potential function (9) reduces to the hyperelastic model presented by Houlsby et al. (2005).

3.4 Coupled isotropic-hardening law

To follow the structure of the rheological model of Armstrong–Frederic (Fig. 1), the energy function $\mathcal{H}(\boldsymbol{\varepsilon}^{\mathrm{p_e}})$ in the "hardening" spring is assumed to have the same functional form as the energy function $W(\boldsymbol{\varepsilon}^{\mathrm{e}})$. The hardening law is thus defined as the following equation:

$$\mathcal{H}(\boldsymbol{\varepsilon}^{\mathrm{p_e}}) \coloneqq \frac{\tilde{\lambda} - \tilde{\kappa}}{2} p_{\mathrm{ref}} \exp\Omega^{\mathrm{p}} \tag{11}$$

where

$$\Omega^{\mathrm{p}} \coloneqq \frac{\varepsilon_{\mathrm{v}}^{\mathrm{p_e}}}{\tilde{\lambda} - \tilde{\kappa}} + \frac{\beta\overline{m}}{\tilde{\lambda} - \tilde{\kappa}}\boldsymbol{e}^{\mathrm{p_e}}:\boldsymbol{e}^{\mathrm{p_e}}. \tag{12}$$

Here, β is a material parameter for controlling the speed of rotation of the yield surface, and $\overline{m}$ is the stress ratio of the rotational limit surface (Hashiguchi, 1998).

From Eq. (7), the volumetric strain of the inelastic part of the plastic strain $\varepsilon_{\mathrm{v}}^{\mathrm{p_i}}$ is always zero. Therefore, for a purely isotropic loading ($\varepsilon_{\mathrm{s}}^{\mathrm{p_e}} = 0$), the preconsolidation pressure p_{c} can be written in the form

$$p_{\mathrm{c}} = 2\bar{p} = p_{\mathrm{ref}} \exp\left(\frac{\varepsilon_{\mathrm{v}}^{\mathrm{p}}}{\tilde{\lambda} - \tilde{\kappa}}\right) \tag{13}$$

This implies that the isotropic consolidation behavior of the proposed model (11) corresponds to that of the Cam-clay-type model in the $\ln p$–$\ln v$ space, as shown in Fig. 3.

From Eqs. (6), (11), and (12), the rotational axis $\bar{\boldsymbol{\eta}}$ is given by the strain $\boldsymbol{\varepsilon}^{\mathrm{p_e}}$ as

$$\bar{\boldsymbol{\eta}} = \frac{\operatorname{dev}(\boldsymbol{\chi})}{\bar{p}} = 2\beta\bar{m}\boldsymbol{e}^{\mathrm{p_e}} \tag{14}$$

At the critical state, the rate of the rotational axis $\dot{\bar{\boldsymbol{\eta}}}$ can be written from Eqs. (8) and (14) as

$$\dot{\bar{\boldsymbol{\eta}}} = 2\beta\bar{m}(\dot{\boldsymbol{e}}^{\mathrm{p}} - \dot{\boldsymbol{e}}^{\mathrm{p_i}}) = 2\beta\dot{\gamma}\left(\bar{m}\frac{\boldsymbol{\eta}-\bar{\boldsymbol{\eta}}}{\|\boldsymbol{\eta}-\bar{\boldsymbol{\eta}}\|} - \bar{\boldsymbol{\eta}}\right) \tag{15}$$

The direction of the rotational axis is the same as the rotational hardening law proposed by Hashiguchi and Chen (1998).

3.5 Subloading surface model

To express the behavior of the overconsolidated soils, we apply the subloading concept (Hashiguchi, 1977) to Eq. (8) as follows:

$$f(\boldsymbol{\sigma},\boldsymbol{\chi},R) \coloneqq \frac{\|\boldsymbol{\eta}-\bar{\boldsymbol{\eta}}\|^2}{m^2 - \|\bar{\boldsymbol{\eta}}\|^2} + 1 - \frac{2R\bar{p}}{p} \tag{16}$$

where $1/R$ represents the overconsolidation ratio. The evolution law of R (Hashiguchi, 2009) is given in this study as

$$\dot{R} = u\cot\left(\frac{\pi R}{2}\right)\|\dot{\varepsilon}^{\mathrm{p}}\| = u\cot\left(\frac{\pi R}{2}\right)\dot{\gamma}. \tag{17}$$

4 RETURN MAPPING

In this section, we present a return mapping algorithm to achieve a highly accurate integration of the proposed hyperelasto-plastic constitutive equations.

4.1 Elastic predictor

Assuming only elastic deformation for a given strain increment $\Delta\boldsymbol{\varepsilon}$ (freezing plastic flow), we obtain

$$\boldsymbol{\varepsilon}^{\mathrm{p,tr}} = \boldsymbol{\varepsilon}_n^{\mathrm{p}}, \qquad \boldsymbol{\varepsilon}^{\mathrm{p_i,tr}} = \boldsymbol{\varepsilon}_n^{\mathrm{p_i}}, \qquad R^{\mathrm{tr}} = R_n \tag{18}$$

where $\boldsymbol{\sigma}^{\mathrm{tr}}$ and $\boldsymbol{\chi}^{\mathrm{tr}}$ are given, respectively, as

$$\boldsymbol{\sigma}^{\mathrm{tr}} = \nabla W(\boldsymbol{\varepsilon} - \boldsymbol{\varepsilon}^{\mathrm{p,tr}}), \text{ and } \boldsymbol{\chi}^{\mathrm{tr}} = \nabla\mathcal{H}(\boldsymbol{\varepsilon}^{\mathrm{p,tr}} - \boldsymbol{\varepsilon}^{\mathrm{p_i,tr}}) \tag{19}$$

The loading/unloading condition can be determined by the trial yield function $f^{\mathrm{tr}} = f(\boldsymbol{\sigma}^{\mathrm{tr}},\boldsymbol{\chi}^{\mathrm{tr}},R^{\mathrm{tr}})$. When $f^{\mathrm{tr}} \le 0$, as only elastic deformation is assumed, variables except R are adopted as the updated values at t_{n+1}, and R is calculated such that $f = 0$ is satisfied. Meanwhile, when $f^{\mathrm{tr}} > 0$, because plastic deformation has occurred, it is necessary to follow the plastic corrector step as described in the next section.

4.2 Plastic corrector

Applying the backward Euler method to the flow rules (7), we define the unknown variable vector $\boldsymbol{x}$ and the residual vector $\boldsymbol{r}(\boldsymbol{x})$, respectively, as

$$\boldsymbol{x} \coloneqq \begin{Bmatrix} \boldsymbol{\sigma} \\ \boldsymbol{\chi} \\ \Delta\gamma \end{Bmatrix}, \qquad \boldsymbol{r}(\boldsymbol{x}) \coloneqq \begin{Bmatrix} \boldsymbol{\varepsilon}^{\mathrm{p}} - \boldsymbol{\varepsilon}_n^{\mathrm{p}} - \Delta\gamma\boldsymbol{N} \\ \boldsymbol{\varepsilon}^{\mathrm{p_i}} - \boldsymbol{\varepsilon}_n^{\mathrm{p_i}} - \Delta\gamma\bar{\boldsymbol{N}} \\ f(\boldsymbol{\sigma},\boldsymbol{\chi},R) \end{Bmatrix} \tag{20}$$

To solve the nonlinear equation $\boldsymbol{r}(\boldsymbol{x}) = \boldsymbol{0}$, the Newton–Raphson method is employed using the following:

$$\delta\boldsymbol{x}_k = -\boldsymbol{A}^{-1}\cdot\boldsymbol{r}(\boldsymbol{x}_k), \qquad \boldsymbol{A} = \frac{\partial\boldsymbol{r}(\boldsymbol{x}_k)}{\partial\boldsymbol{x}} \tag{21}$$

where $\delta\boldsymbol{x}_k$ is the corrector vector. This iteration is conducted to update $\boldsymbol{x}_{k+1}$ until $\|\boldsymbol{r}\| < \mathrm{TOL}$.

5 CONSISTENT TANGENT MODULUS

The nonlinear equation $\boldsymbol{r}(\boldsymbol{x}) = \boldsymbol{0}$ can be rewritten as

$$\boldsymbol{r}(\boldsymbol{x}(\boldsymbol{\varepsilon}),\boldsymbol{\varepsilon}) = \boldsymbol{0}. \tag{22}$$

The total derivative of Eq. (22) is given by

$$\frac{\partial\boldsymbol{r}}{\partial\boldsymbol{\varepsilon}} = \left.\frac{\partial\boldsymbol{r}}{\partial\boldsymbol{\varepsilon}}\right|_{\boldsymbol{x}} + \left.\frac{\partial\boldsymbol{r}}{\partial\boldsymbol{x}}\right|_{\boldsymbol{\varepsilon}}\cdot\frac{\partial\boldsymbol{x}}{\partial\boldsymbol{\varepsilon}} = \left.\frac{\partial\boldsymbol{r}}{\partial\boldsymbol{\varepsilon}}\right|_{\boldsymbol{x}} + \boldsymbol{A}\cdot\frac{\partial\boldsymbol{x}}{\partial\boldsymbol{\varepsilon}} = \boldsymbol{0} \tag{23}$$

Therefore, the consistent tangent modulus $\partial\boldsymbol{\sigma}/\partial\boldsymbol{\varepsilon}$ can be obtained by solving Eq. (23):

$$\frac{\partial\boldsymbol{x}}{\partial\boldsymbol{\varepsilon}} = \begin{Bmatrix} \dfrac{\partial\boldsymbol{\sigma}}{\partial\boldsymbol{\varepsilon}} \\ \dfrac{\partial\boldsymbol{\chi}}{\partial\boldsymbol{\varepsilon}} \\ \dfrac{\partial\Delta\gamma}{\partial\boldsymbol{\varepsilon}} \end{Bmatrix} = -\boldsymbol{B}\cdot\left.\frac{\partial\boldsymbol{r}}{\partial\boldsymbol{\varepsilon}}\right|_{\boldsymbol{x}} = -\begin{Bmatrix} \boldsymbol{B}_{11}+\boldsymbol{B}_{12} \\ \boldsymbol{B}_{21}+\boldsymbol{B}_{22} \\ \boldsymbol{B}_{31}+\boldsymbol{B}_{32} \end{Bmatrix} \tag{24}$$

where $\boldsymbol{B} = \boldsymbol{A}^{-1}$. Because we use the Jacobian $\boldsymbol{A}$ in which the iteration is completed, the existence of $\boldsymbol{A}^{-1}$ is guaranteed.

6 STRESS-CONTROLLED CYCLIC SIMPLE SHEARING SIMULATIONS

In this section, we set the following problem to perform stress-controlled cyclic simple shearing simulations based on a study by Borja et al. (2001):

$$\boldsymbol{R} \coloneqq \boldsymbol{\sigma}^* - \tilde{\boldsymbol{\sigma}}, \qquad \tilde{\boldsymbol{\sigma}} = \boldsymbol{\sigma}(\boldsymbol{\varepsilon}) + \zeta\ \mathrm{tr}(\boldsymbol{\varepsilon})\boldsymbol{1} \tag{25}$$

where $\zeta \gg 0$ is a penalty parameter that should be sufficiently large to satisfy $\mathrm{tr}(\boldsymbol{\varepsilon}) \to 0$. We use $\zeta = 10^8$ kPa in this study. The nonlinear equation $\boldsymbol{R} = \boldsymbol{0}$ can be solved by the Newton–Raphson method as

$$\mathrm{d}\boldsymbol{\varepsilon}_k = -\left[\frac{\partial\boldsymbol{R}(\boldsymbol{\varepsilon}_k)}{\partial\boldsymbol{\varepsilon}}\right]^{-1}\cdot\boldsymbol{R}_k \tag{26}$$

where

$$\frac{\partial\boldsymbol{R}(\boldsymbol{\varepsilon}_k)}{\partial\boldsymbol{\varepsilon}} = -\frac{\partial\boldsymbol{\sigma}(\boldsymbol{\varepsilon}_k)}{\partial\boldsymbol{\varepsilon}} - \zeta\boldsymbol{1}\otimes\boldsymbol{1} \tag{27}$$

The consistent tangent modulus (24) should be used for $\partial\boldsymbol{\sigma}/\partial\boldsymbol{\varepsilon}$ in Eq. (27) to preserve the asymptotic rate of the quadratic convergence of the iterations.

From the initial stress $\sigma_{11} = \sigma_{22} = \sigma_{33} = 350$ kPa, cyclic simple shearing is applied with stress increment $\Delta\sigma_{12} = \pm 40$ kPa by 360 and 3600 steps in nine cycles (Fig. 3). From Fig. 4(a), the soil loses its mean stress p owing to cyclic shearing at the beginning of the simulation, and finally exhibits cyclic mobility. Figure 4(b) shows that the large deviatoric strain suddenly occurs during the cyclic mobility. Additionally, from Fig. 4, the calculation results are highly accurate even for large increments.

7 CONCLUSIONS

An infinitesimal constitutive model for soils that considered induced anisotropy was formulated based on the finite strain framework proposed by Lion (2000). In the formulation, we proposed the hyperelastic constitutive model and the hardening law which could describe both isotropic and rotational hardenings based on the kinematic hardening law of Armstrong and Frederick

Table 1. Material parameters used in the stress-controlled cyclic simple shearing simulations.

Parameter and symbol	Value
Reference mean stress p_{ref}	98.0 kPa
Elastic shear modulus μ_{ref}	6000.0 kPa
Elastic volumetric–deviatoric parameter α	40.0
Swelling index $\tilde{\kappa}$	0.01
Compression index $\tilde{\lambda}$	0.11
Critical state stress ratio M	1.1
Stress ratio of rotational limit surface $\bar{M}$	1.0
Parameter of subloading surface u	0.96
Parameter of anisotropy β	18.0

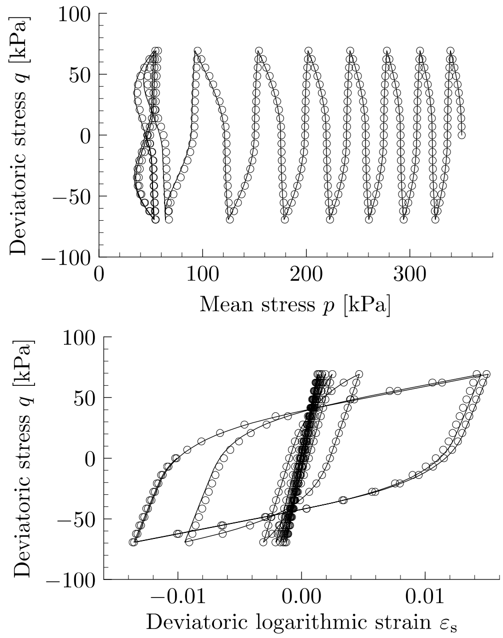

Fig. 4. Stress-controlled cyclic simple shearing simulation (line: 3600 steps, plot: 360 steps): (a) stress path, (b) deviatoric stress–deviatoric strain relationship.

(1966). To apply the Armstrong–Frederick kinematic hardening law to the constitutive model for soils, we developed a new approach to describe the anisotropic behavior of soils by the back stress.

From the stress-controlled cyclic simple shearing simulations, the proposed model could predict the stress-induced anisotropy behaviors of soils.

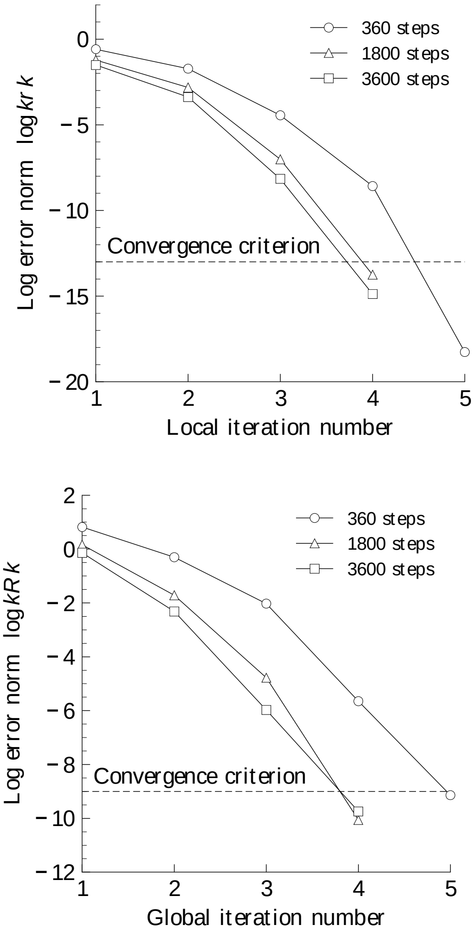

Fig. 5. Convergence properties at the final step: (a) return mapping, (b) global iteration.

REFERENCES

Armstrong, P. J. and Frederick, C. (1966). A mathematical representation of the multiaxial bauschinger effect. CEBG Report RD/B/N, 731.

Borja, R. I., Lin, C. H., and Montans, F. J. (2001). Cam-clay plasticity, Part IV: Implicit integration of anisotropic bounding surface model with nonlinear hyperelasticity and ellipsoidal loading function. Computer Methods in Applied Mechanics and Engineering, 190(26–27), 3293–3323.

Borja, R. I., Tamagnini, C., and Amorosi, A. (1997). Coupling Plasticity and Energy-Conserving Elasticity Models for Clays. Journal of Geotechnical and Geoenvironmental Engineering, 123(10), 948–957.

Chida, Y., Yamakawa, Y., Hashiguchi, K., and Ikeda, K. (2013). Subloading surface Cam-clay model with anisotropic rotational hardening for finite strains based on multiplicative decomposition of plastic deformation gradient tensor. Journal of JSCE, Ser. A2, 69 (in Japanese).

Dafalias, Y. F., 1986. An anisotropic critical state soil plasticity model. Mechanics Research Communications 13(6), 341–347.

Dettmer, W. and Reese, S. (2004). On the theoretical and numerical modelling of Armstrong–Frederick kinematic hardening in the finite strain regime. Computer Methods in Applied Mechanics and Engineering 193(1–2), 87–116.

Hashiguchi, K. (2009). Elastoplasticity Theory (Vol. 42). Berlin, Heidelberg: Springer Berlin Heidelberg.

Hashiguchi, K. and Chen, Z.-P. (1998). Elastoplastic constitutive equation of soils with the subloading surface and the rotational hardening. International Journal for Numerical and Analytical Methods in Geomechanics, 22(3), 197–227.

Hashiguchi, K. and Ueno, M. (1977). Elastoplastic constitutive laws of granular materials, constitutive equations of soils. In 9th International Conference on Soil Mechanics and Foundation Engineering, Special Session 9, 73–82.

Lion, A. (2000). Constitutive modelling in finite thermoviscoplasticity: A physical approach based on nonlinear rheological models. International Journal of Plasticity, 16(5), 469–494.